

Analysis Of Technological Operations For The Development Of Aluminum-Based High-Strength Nanostructured Materials (Coatings)

Shohruh Hudoykulov

Tashkent State Technical University, 100095, University str. 2, Tashkent, Uzbekistan

Sherzod Tashbulatov

Tashkent State Technical University, 100095, University str. 2, Tashkent, Uzbekistan

Received: 26 October 2025; **Accepted:** 15 November 2025; **Published:** 21 December 2025

Abstract: The development of aluminum-based high-strength nanostructured materials and coatings is essential for advanced surface engineering applications. Their functional properties strongly depend on the technological operations employed during fabrication. This study analyzes the key technological stages involved in producing aluminum-based nanostructured coatings, including substrate preparation, thin film deposition, anodization, and post-treatment processes. Particular attention is paid to the influence of processing parameters on the formation of nanoscale structures and columnar morphologies. The analysis shows that optimization of technological operations allows effective control of structural characteristics, leading to improved hardness, elastic modulus, and mechanical stability of the coatings. The results demonstrate the potential of optimized aluminum-based nanostructured coatings for use in high-performance engineering and protective applications.

Keywords: Nanostructured coatings, post-treatment processes, elastic modulus, tantalum oxide.

INTRODUCTION:

In recent years, in the field of modern materials science and engineering modification of surfaces, there has been a significant increase in interest in the development of solid nanostructural materials and coatings with an aluminum base. Aluminum and its alloys are widely used in aviation, automotive, energy, microelectronics and other high-tech industries due to their properties such as low density, high specific strength, good thermal and electrical conductivity, and stability to corrosion [1-6]. At the same time, the mechanical and operational properties of traditional aluminum materials do not fully satisfy some engineering requirements, which makes it necessary to strengthen them at the nanostructural level.

The sequence of technological operations used in the formation of aluminum-based nanostructural coatings and their interrelationships are one of the main factors determining the final structure and functional properties of the coating. In particular, the

processes of preparation of a metal base, deposition of thin layers, anodizing and reanodizing, as well as the stages of heat and electrochemical processing, have a direct effect on the formation mechanisms of nanostructure. Through an in-depth analysis of each of these technological operations, it is possible to control the micro-and nanomorphology of the coating, the mechanical strength and the duration of its service life [7-11].

Experimental Studies

The results of investigations into the formation and modification processes of porous anodic aluminum oxide (AAO) matrices, as well as methods for the electrochemical oxidation of tantalum through AAO pores and the formation of columnar nanostructures within these pores, served as the basis for developing a preliminary technological route for producing nanostructured composite coatings with specified structural parameters and geometric dimensions [12-14]. These coatings are intended for strengthening

and protecting products made of aluminum and aluminum alloys against external influences [15]. The draft technology was developed and tested on aluminum rolled blanks. The schematic technological operations for producing the new reinforcing nanostructured coatings are presented in Table 1.

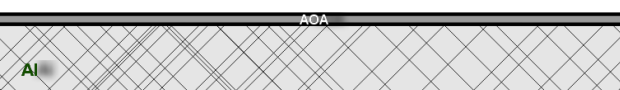
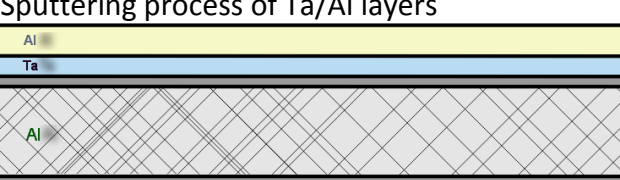
Initially, primary blanks with dimensions of 60×48 mm were stamped from aluminum rolled stock with a thickness of $2000 \mu\text{m}$ (99.95% purity). After multiple polishing steps, thermo-straightening was carried out at 350°C under a pressure of approximately 10^7 Pa [16]. Subsequently, the blanks were cleaned in a chromium-containing solution ($\text{CrO}_3:\text{H}_2\text{SO}_4$ at a ratio of 1:100) at a temperature of $18\text{--}20^\circ\text{C}$ for 2–3 min to remove surface contaminants. The samples were then rinsed in distilled water and dried with hot air at

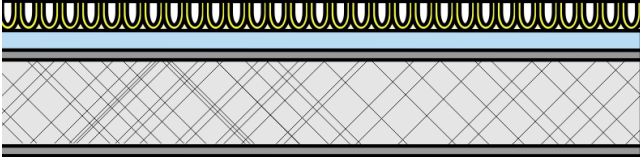
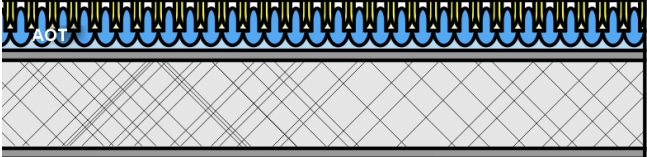
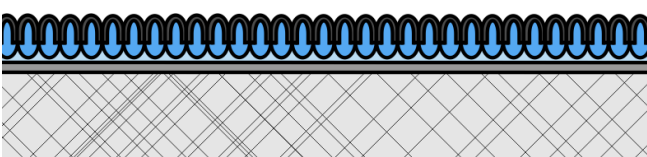
$100 \pm 5^\circ\text{C}$ for 5 min [17].

To remove micro-asymmetries from the aluminum surface, an electrochemical polishing operation was performed in an electrolyte consisting of 65% perchloric acid and 99.5% acetic acid in a 22%:78% ratio, at an electrolyte temperature of $7\text{--}9^\circ\text{C}$. The process was conducted under continuous stirring at an applied voltage of 25–27 V and a current density of 250–300 mA/cm^2 . The anodic treatment time ranged from 30 to 60 s [18–20]. After electrochemical polishing, the samples were thoroughly rinsed in running and distilled water, dried with compressed air, and finally dried in a thermostat at 160°C for 20 min.

DISCUSSION

Table 1. Sequence of technological operations for the fabrication of aluminum-based high-strength nanostructured materials (coatings).

No	Experimental operation procedure and schematic diagram	Experimental procedure
1	Preparation of an Al-containing experimental sample 	The sample was chemically cleaned under a pressure of 10^7 Pa at a temperature of 350°C in a chromium-containing solution. The cleaning process ($\text{CrO}_3:\text{H}_2\text{SO}_4$ in a 1:100 ratio) was carried out at a temperature of $18\text{--}20^\circ\text{C}$ for 2–3 min.
2	Chemical cleaning 	Electrochemical polishing (brightening) was performed using a solution of 65% perchloric acid and 99.5% acetic acid in a 22%:78% ratio at a temperature of $7\text{--}9^\circ\text{C}$, under an applied voltage of 25–27 V and a current density of 250–300 mA/cm^2 , for a duration of 30–60 s.
3	Formation of an adhesive protective layer 	The anodization process was carried out in a 0.5 M aqueous oxalic acid solution at a temperature of $T = 14 \pm 0.5^\circ\text{C}$, to a depth of $0.5 \mu\text{m}$, under a constant voltage of 50 V, with preliminary potential scanning at a rate of 10 V/s.
4	Sputtering process of Ta/Al layers 	Tantalum with a thickness of $0.5 \pm 0.05 \mu\text{m}$ was deposited onto the sample surface by the magnetron sputtering method in the chamber of the "Oratoria-9" setup under a pressure of $P = 900 \text{ Pa}$, at a temperature of $T = 250^\circ\text{C}$, with a

		sputtering current of $I = 0.9 \text{ A}$ and an accelerating voltage of $U = 6 \text{ kV}$.
5	Anodization of Al 	The electrochemical anodization of aluminum was carried out in a 0.4 M oxalate solution at an applied voltage of $E_a = 53 \text{ V}$ and a current density of $j = 10 \text{ mA/cm}^2$, at a temperature of $T = 10\text{--}12 \text{ }^\circ\text{C}$, until the current density decreased to $20 \mu\text{A/cm}^2$.
6	Anodization and re-anodization of Ta 	Anodization was carried out in a 0.1 M citric acid solution by increasing the voltage at a rate of 1 V/s up to 220 V and maintaining the process for 18 min until the current density decreased to $20 \mu\text{A/cm}^2$. The re-anodization process was performed in a 0.5 M $\text{H}_3\text{BO}_3 + 0.05 \text{ M Na}_2\text{B}_4\text{O}_7$ electrolyte under an applied voltage of $E = 420 \text{ V}$, with an anodization current density of $j = 500 \mu\text{A/cm}^2$. The voltage was increased at a rate of 2 V/s up to 420 V, and the process was maintained for 30 min until the current density decreased to $40 \mu\text{A/cm}^2$.
7	Application of the PVDF planarization process to the AAO/ATO structure 	The selective removal of the AAO layer from the columnar structures in solution was carried out using an electrolyte containing chromium trioxide (20 g/L) and orthophosphoric acid (60 g/L), diluted with distilled water to a total volume of 1 L, at a temperature of 60 °C. PVDF was applied to the structure with a thickness of 0.2–0.45 μm . The spreading time was 6 min, while the film formation time was 30 s, at a rotation speed of 3200 rpm. Drying of the PVDF layer was performed at a temperature of $T = 80\text{--}100 \text{ }^\circ\text{C}$ for 45 min.

The prepared sample blanks were mounted in special holders inside a vacuum chamber and heated to a temperature of $230 \pm 20 \text{ }^\circ\text{C}$. Subsequently, double-sided tantalum deposition was carried out using the magnetron sputtering method on the production line of the Oratoria-9M system. In the Oratoria-9 setup, a

tantalum layer with a thickness of $0.5 \pm 0.05 \mu\text{m}$ was deposited onto the working surface under a chamber pressure of $P = 900 \text{ Pa}$, at a temperature of $T = 250 \text{ }^\circ\text{C}$, with a sputtering current of $I = 0.9 \text{ A}$ and an accelerating voltage of $U = 6 \text{ kV}$. After that, an aluminum layer with a thickness of $1.5 \pm 0.05 \mu\text{m}$ was

deposited onto the tantalum surface.

The deposited aluminum layer was anodized in a 0.4 M oxalic acid solution at an anodization voltage of $E_a = 53$ V, with an anodization current density not exceeding $j = 10$ mA/cm², and an electrolyte temperature of $T = 10\text{--}12$ °C. The formation of tantalum columns was achieved by high-voltage re-anodization through the pores of the formed anodic aluminum oxide. The re-anodization process was carried out in a 0.5 M H_3BO_3 + 0.05 M $Na_2B_4O_7$ solution at an applied voltage of $E = 420$ V and an anodization current density not exceeding $j = 500$ μ A/cm².

After electrochemical anodization, the porous AAO layer was selectively removed from the columnar structures using a solution containing chromium trioxide (20 g/L) and orthophosphoric acid (60 g/L), diluted with distilled water to a total volume of 1 L, at a temperature of 60 °C for 20 min. As a result of this operation, a planar AAO/ATO structure was formed. The total thickness of the coating was approximately 1.2 μ m.

CONCLUSION

All the described methods are implemented using specialized equipment, which makes their practical realization relatively simple. This approach enables controlled single-stage or multistage formation of nanostructured coatings. The experimental procedures carried out using this method comply with environmental requirements. In addition to being cost-effective, the proposed approach allows the fabrication of materials with high wear resistance, as well as enhanced thermal and corrosion resistance.

REFERENCES

1. Ganjam, S., Wang, Y., Lu, Y., Banerjee, A., Lei, C. U., Krayzman, L., Kisslinger, K., Zhou, C., Li, R., Jia, Y., Liu, M., Frunzio, L., & Schoelkopf, R. J. (2024). Surpassing millisecond coherence in on chip superconducting quantum memories by optimizing materials and circuit design. *Nature Communications*, 15(1). <https://doi.org/10.1038/s41467-024-47857-6>
2. Nickel, M. R., Melligan, G., McMullen, T. P. W., & Burrell, R. E. (2019). The effect of chemical additives in phosphoric acid anodization of aluminum-tantalum thin films. *Thin Solid Films*, 685. <https://doi.org/10.1016/j.tsf.2019.06.033>
3. Okamoto, H. (2010). Al-Ta (aluminum-tantalum). In *Journal of Phase Equilibria and Diffusion* (Vol. 31, Issue 6). <https://doi.org/10.1007/s11669-010-9786-5>
4. El-Eskandarany, M. S., Aoki, K., & Suzuki, K. (1992). Formation of amorphous aluminum tantalum nitride powders by mechanical alloying. *Applied Physics Letters*, 60(13). <https://doi.org/10.1063/1.107251>
5. Turakhodjaev, N. D., Tursunbaev, S. A., Odilov, F. U., Zokirov, R. S., & Kuchkarova, M. Kh. (2020). Vliyanie uslovii legirovaniya na svoistva belykh chugunov [Influence of alloying conditions on the properties of white cast irons]. In *Tekhnika i tekhnologii mashinostroeniya* (pp. 63–68).
6. Okayasu, M., Takeuchi, S., & Shiraishi, T. (2013). Corrosion and mechanical properties of cast aluminium alloys. *International Journal of Cast Metals Research*, 26(6), 319–329. <https://doi.org/10.1179/1743133613Y.0000000067>
7. Drevet, R., Souček, P., Mareš, P., Ondračka, P., Fekete, M., Dubau, M., & Vašina, P. (2025). Influence of oxygen flow on the structure, chemical composition, and dielectric strength of Al_xTa_yO_z thin films deposited by pulsed-DC reactive magnetron sputtering. *Surface and Coatings Technology*, 498. <https://doi.org/10.1016/j.surfcoat.2025.131865>
8. Tursunbaev, S., Turakhodjaev, N., Turakhujaeva, S., Ozodova, S., Hudoykulov, S., & Turakhujaeva, A. (2022). Reduction of gas porosity when alloying A000 grade aluminum with lithium fluoride. *IOP Conference Series: Earth and Environmental Science*, 1076(1), 012076. <https://doi.org/10.1088/1755-1315/1076/1/012076>
9. Gao, Y. X., Yi, J. Z., Lee, P. D., & Lindley, T. C. (2004). The effect of porosity on the fatigue life of cast aluminium–silicon alloys. *Fatigue & Fracture of Engineering Materials & Structures*, 27(7), 559–570. <https://doi.org/10.1111/j.1460-2695.2004.00763.x>
10. Roven, H. J., Nesbø, H., Werenskiold, J. C., & Seibert, T. (2005). Mechanical properties of aluminium alloys processed by severe plastic deformation: Comparison of different alloy systems and possible product areas. *Materials Science and Engineering: A*, 410–411, 426–429. <https://doi.org/10.1016/j.msea.2005.08.153>
11. Skejić, D., Dokšanović, T., Čudina, I., & Mazzolani, F. M. (2021). The basis for reliability-based mechanical properties of structural aluminium alloys. *Applied Sciences*, 11(10), 4485. <https://doi.org/10.3390/app11104485>
12. Anusionwu, B. C., Adebayo, G. A., & Madu, C. A. (2009). Thermodynamics and surface properties

of liquid Al–Ga and Al–Ge alloys. *Applied Physics A*, 97(3), 533–541.
<https://doi.org/10.1007/s00339-009-5334-4>

13. Miura, K., & Omi, K. (2024). Near-infrared light emission from aluminum-doped tantalum-oxide thin films prepared using a simple co-sputtering method. *Results in Physics*, 57.
<https://doi.org/10.1016/j.rinp.2024.107389>
14. Hu, B. Q., Wang, X. M., Zhou, T., Zhao, Z. Y., Wu, X., & Chen, X. L. (2001). Transmittance and refractive index of the lanthanum strontium aluminium tantalum oxide crystal. *Chinese Physics Letters*, 18(2).
<https://doi.org/10.1088/0256-307X/18/2/342>
15. Umarov, T. U., Tursunbaev, S. A., & Mardonov, U. T. (2018). Novye tekhnologicheskie vozmozhnosti povysheniya ekspluatatsionnoi nadezhnosti instrumentov dlya obrabotki kompozitsionnykh materialov [New technological possibilities for improving the operational reliability of tools for machining composite materials]. In *Tekhnika i tekhnologii mashinostroeniya* (pp. 70–74).
16. Hirsch, J., Skrotzki, B., & Gottstein, G. (Eds.). (2008). *Aluminium alloys: The physical and mechanical properties* (Vol. 1). Wiley-VCH.
17. Tursunbaev, S., Umarova, D., Kuchkorova, M., & Baydullaev, A. (2022). Study of machining accuracy in ultrasonic elliptical vibration cutting of alloyed iron alloy carbon with germanium. *Journal of Physics: Conference Series*, 2176(1), 012053. <https://doi.org/10.1088/1742-6596/2176/1/012053>
18. Sarvar, T., Nodir, T., Mardonov, U., Saydumarov, B., Kulmuradov, D., & Boltaeva, M. (2024). Effects of germanium (Ge) on hardness and microstructure of Al–Mg, Al–Cu, and Al–Mn system alloys. *International Journal of Mechatronics and Applied Mechanics*, (16), 179–184.
19. Lu, Q., Skeldon, P., Thompson, G. E., Habazaki, H., & Shimizu, K. (2005). Composition and density of non-thickness-limited anodic films on aluminium and tantalum. *Thin Solid Films*, 471(1–2).
<https://doi.org/10.1016/j.tsf.2004.04.061>
20. Mann, A. E., & Newkirk, J. W. (2023). Fundamental Effects of Al and Ta on Microstructure and Phase Transformations in the Al–Cr–Mo–Ta–Ti Refractory Complex Concentrated Alloy System. *Advanced Engineering Materials*, 25(9).
<https://doi.org/10.1002/adem.202201449>